Solar Neutrino Physics with Super-Kamiokande

Michael B Smy* for the Super-Kamiokande-Collaboration

University of California, Irvine, 3117 Frederick Reines Hall, Irvine, California 92697-4575

***Abstract*. Precise studies of solar ^{8}B neutrinos provided the first evidence that the deficit in the solar neutrino flux observed by various detectors compared to the predictions of solar models is caused by flavor oscillations of solar neutrinos and also determined the oscillation parameters. These parameters predict a transition at around 3 Mev between the vacuum oscillations of low energy to the matter-dominated oscillations for the higher energy neutrinos. Thus far there is no observation of either this transition or the day/night asymmetry – the only direct demonstration of matter effects on solar neutrino oscillations. Super-Kamiokande's past solar neutrino measurements and the efforts towards a lower analysis threshold and a more precise measurement of the day/night asymmetry are presented.**

***Keywords*: sun, neutrinos, neutrino oscillation**

I. Introduction

Super-Kamiokande, a 50kton cylindrical water Cherenkov detector located about 3 km w.e. underground, observes solar neutrinos via elastic scattering off electrons. About 11,000 20" photomultiplier tubes view the innermost 32 kton and yield about six detected photo-electrons per MeV of electron energy. As a consequence only the high energy ^{8}B and *hep* neutrinos can be observed. However, the direction and energy of the recoiling electrons are reconstructed, so neutrino interactions are recorded in real-time and point back to the sun. Also, the large fiducial mass of the innermost 22.5kton of the detector results in a large solar neutrino interaction rate of about 15 events/day above 5 MeV after event selection. Consequently, the first phase of the experiment, Super-Kamiokande-I collected about 22,000 solar neutrino events in about five years – by far the largest sample of solar neutrinos in the world. Since all solar neutrino flavors undergo elastic scattering with electrons – although the cross section for the electron flavor is enhanced – a comparison of the elastic scattering rate at Super-Kamiokande with the charged-current interaction rate of purely electron-flavored solar neutrinos with deuterons at the Sudbury neutrino observatory [1] provided the first evidence of solar neutrino flavor transformation.

II. Super-Kamiokande-I Results

Super-Kamiokande-I measured the ^{8}B neutrino flux to be $\Phi = 2.35 \pm 0.02(\text{stat}) \pm 0.08(\text{syst}) \times 10^6/\text{cm}^2\text{sec}$ [2]. The (total) energy threshold for the recoil electrons was 5 MeV. There appears to be no significant distortion in the recoil electron spectrum (see Figure 1). The solar neutrino interaction rate was searched for various time variations; the only significant time variation found is caused by the 1.7% orbital eccentricity of the Earth producing a 7% variation simply from the inverse square radius law. From the solar neutrino data, the eccentricity was measured to be $2.1 \pm 0.3\%$(syst), the perihelion shift seen in the neutrino data with respect to the true perihelion is 13 ± 18 days. Among the time variations the so-called day/night asymmetry $A_{DN} = \frac{\Phi_D - \Phi_N}{0.5(\Phi_D + \Phi_N)}$ was most carefully studied; a non-zero value would be a sign of Earth matter effects on solar neutrino oscillation (usually a regeneration of electron-flavor neutrinos). The straight day/night asymmetry was measured to be $A_{DN} = -0.021 \pm 0.020(\text{stat}) \pm 0.012(\text{syst})$. Also, a fit to the amplitude of the expected day/night variation using the solar neutrino oscillation parameters in the Large Mixing Angle region yields $-0.017 \pm 0.016(\text{stat}) \pm 0.012(\text{syst}) \pm 0.0004(\text{osc})$ when expressed as a day/night asymmetry.

III. Super-Kamiokande-II Results

The second phase, Super-Kamiokande-II, confirmed the results of Super-Kamiokande-I. Solar neutrinos were detected for recoil electrons above 7 MeV of (total) energy and the ^{8}B neutrino flux of $\Phi = 2.38 \pm 0.05(\text{stat}) \pm 0.015(\text{syst}) \times 10^6/\text{cm}^2\text{sec}$ [3] agrees with Super-Kamiokande-I much better than expected even from statistical uncertainties alone (see Figure 1). This is particularly remarkable since Super-Kamiokande-II has only 46.5% of the photomultiplier tubes of Super-Kamiokande-I, those photo detectors are enclosed in blast shields which remove a few percent of the light and add radioactive background. Furthermore, the entire analysis had to be rebuild including event reconstruction, event selection and detector calibration. Like Super-Kamiokande-I, the second phase found no distortions (see Figure 1) in the recoil electron spectrum. The day/night asymmetry was measured to be $A_{DN} = -0.063 \pm 0.042(\text{stat}) \pm 0.037(\text{syst})$ – also in good agreement with Super-Kamiokande-I. There is no significant time variation of the elastic scattering rate of any kind, except the seasonal variation due to the inverse square radius law. Super-Kamiokande-I and II together span an entire 11 year solar cycle, there's no significant dependence of the ^{8}B solar neutrino flux on this cycle (see Figure 2).

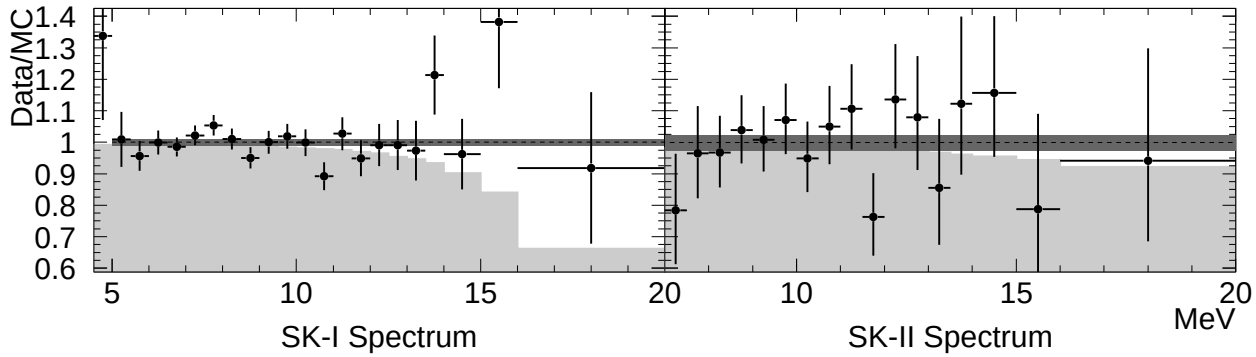

Fig. 1. Recoil Electron Spectral Distortion for Super-Kamiokande-I (Left) and Super-Kamiokande-II (Right). The ratio of the measured and the expected solar neutrino elastic scattering rate from a ^{8}B neutrino flux of 2.33×10^6/cm^{2}sec and a *hep* neutrino flux of 15×10^3/cm^{2}sec is displayed. The shaded area is the contribution from just the ^{8}B neutrino flux. The dark-colored band represents the value and statistical uncertainty of the combined rate 5-20 MeV (7-20 MeV).

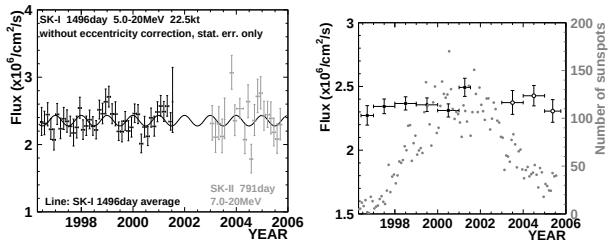

Fig. 2. Solar Neutrino Flux Time Dependence (Left) Compared To Sunspot Number (Right).

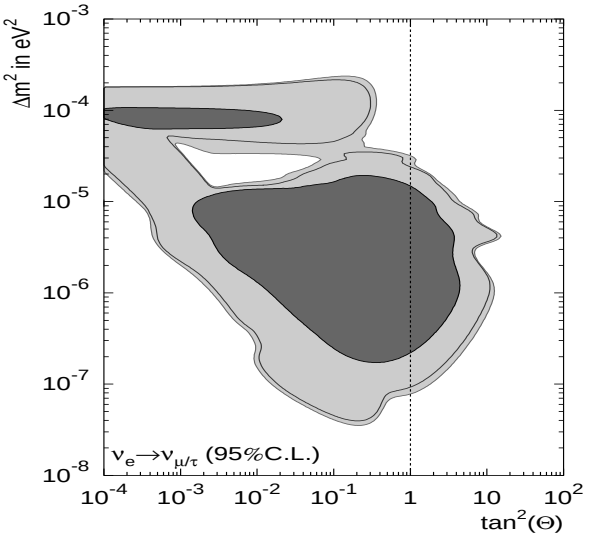

Fig. 3. Excluded Solar Neutrino Oscillation Parameters From Super-Kamiokande-I (Line), Super-Kamiokande-II (Dark Gray Area) and Super-Kamiokande-I+II (Light Gray Area) Data.

IV. Super-Kamiokande-III

The third phase of Super-Kamiokande restored the full number of photomultiplier tubes to the experiment. In spite of the radioactivity introduced by the blast shields, the background level near 5 MeV is significantly lower than Super-Kamiokande-I in the center of the detector due to an improved water circulation pattern which suppresses the transport of Radon to the center. While the trigger efficiency at 5 MeV is 100% (indeed at the very end of Super-Kamiokande-III it was 100% at 4.5 MeV) the hardware trigger threshold does not allow a significant lower analysis threshold than SK-I.

V. Solar Neutrino Oscillations

For ^{8}B neutrinos, solar neutrino oscillations are governed by a MSW resonance [4], i.e. resonant, maximal production of the higher mass eigenstates outside the sun due to the flavor discrimination of the high solar matter density. The absence of sizable earth matter effects and the absence of an energy dependence of the flavor conversion above 5 MeV places strong constraints on the solar mixing angle θ and the solar mass^2 splitting Δm^2; only the so-called "large mixing angle" region (near $\Delta m^2 = 10^{-4}$eV^2 and $\tan^2\theta = 0.5$) is able to explain it. Figure 3 shows a 95% exclusion contour from Super-Kamiokande-I and II data. The large mixing angle region predicts the smallest spectral distortion for ^{8}B neutrinos, but even in that region the flavor conversion has to become energy dependent below 5 MeV. In fact, it undergoes a transition at around 3 MeV to simple, averaged vacuum-driven oscillations. Since the flavor conversion above 5 MeV is around 70%, the averaged vacuum-driven oscillations imply a smaller conversion rate.

VI. Super-Kamiokande-IV Trigger

Last September, the Super-Kamiokande electronics and data acquisition was modernized and redone. To fully take advantage of the lower radioactive background of the center of Super-Kamiokande-III with respect to Super-Kamiokande-I there is no event trigger anymore. Instead, data is acquired continuously and events are extracted by a software trigger system from this data stream.

The data acquisition system produces a clock hardware trigger about every 17 μs. The clock is synchronized to 32,768 steps of the tdc resolution (1.92 tdc counts per ns). The data acquisition computers (called

"mergers") combine 1,344 (about 23ms of data) consecutive hardware triggers into one data block. The blocks overlap by about one ms in time. The hardware triggers are then sent to the software trigger computers and are further processed by organizer computers which sort the events defined by the software triggers by time of acquisition. The computing and storage capacity of this system is exhausted at an energy threshold quite similar to that of Super-Kamiokande-III. However, this software trigger just emulates the trigger hardware of the previous phases: if the number of hit photomultiplier tubes within 200ns exceeds a given value (the threshold), all data nearby in time is saved as an event. The raw tdc counts are used for the coincidence rather than calibrated times.

The new Wide-band Intelligent Trigger system (WIT) on the other hand uses such a simple coincidence only as a rough pre-filter. To transfer the data from the mergers, two ProCurve network switches combine the many "slow" 1Gbit/sec ethernet lines connected to the mergers into four "fast" 10Gbit/sec ethernet lines which feed the four computers of the WIT system. Each WIT computer contains two quad-core 3GHz CPUs and runs independently. WIT processes each data block independently: First, the times and charges of all hit photomultiplier tubes are determined by the raw tdc and adc counts. Then a 230ns search window is defined. From the hit rate outside the window the dark noise level is determined. If the coincidence signal exceeds that level by about 11 hits (this roughly corresponds to 2.5 MeV or 3 MeV) the next filter is applied: the Software Triggered Online Reconstruction of Events (STORE) first selects those hits from the 230ns search window that might be due to light originating from a single vertex. A necessary (although not sufficient) condition for that is, that any given pair of hits must show a time coincidence at least as tight or tighter than the separation of these two photomultiplier tubes. The list of selected hit photomultiplier tubes is constructed using these pair correlations. From this list four-hit combinations are drawn. STORE attempts to use the four arrival times t_i of a four-hit combination to calculate the vertex $(\vec{v}, t)$ that would explain all four hit times given the hit positions $\vec{p}_i$. All vertices that are inside the Super-Kamiokande fiducial volume (two meters inward from any photomultiplier tube) are then checked against *all* members of the list of selected photomultiplier tubes:

$$g = \sum_{|ct_i - |\vec{v}-\vec{p}_i| - ct| < 3m} e^{-\left(\frac{ct_i - |\vec{v}-\vec{p}_i| - ct|}{1m}\right)^2}$$

By construction, the vertex coincidence g must exceed 4; if any g exceeds 6.6, STORE performs a fast vertex fit to *all* the selected hits simultaneously (fitting starts from the set of positions from the four-hit combinations). If this reconstructed vertex is inside the fiducial volume, STORE performs the full, slow maximum likelihood vertex fit to *all* hit photomultiplier tubes in *or near* the 230ns search window taking into account direct, reflected, and scattered light as well as dark noise. If this vertex is still inside the fiducial volume, an event is formed and permanently stored.

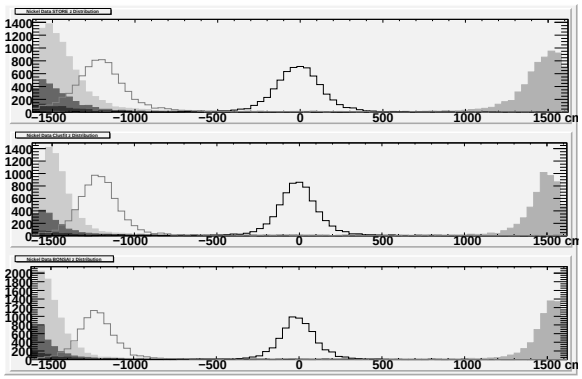

Fig. 4. Test of WIT System with Ni-Cf Calibration Source at Six Positions: (0.4,-0.7,-17.1)m,(0.4,-0.7,-16.1)m, (0.4,-0.7,-15.1)m, (0.4,-0.7,-12)m, (0.4,-0.7,0)m, and (0.4,-0.7,+15.1m). The top panel shows the z-position of the four-hit combination vertex with the largest coincidence g. The middle panel plots the fast vertex reconstruction and the bottom panel the full maximum likelihood vertex fit.

TABLE I
WIT EFFICIENCY MEASURED AT SIX POSITIONS WITH (X,Y)=(0.4,-0.7)M. THE FIRST TWO EFFICIENCY COLUMNS ARE DUE TO THE VERTEX RESOLUTION OF THE FAST FIT WITH RESPECT TO THE MAXIMUM LIKELIHOOD FIT. THE EDGE OF THE FIDUCIAL VOLUME IS $\pm$16.1M.

z in m	ϵ_{fit}(3 MeV)	ϵ_{fit}(4 MeV)	ϵ(3 MeV)	ϵ(4 MeV)
-17.1	61%	60%	56%	57%
-16.1	65%	71%	62%	68%
-15.1	73%	78%	71%	76%
-12	94%	96%	93%	95%
0	86%	93%	84%	92%
+15.1	76%	84%	73%	82%
+16.1	64%	68%	62%	66%

The WIT system was tested with a Ni-Cf source inserted at the positions (0.4,-0.7,-17.1)m,(0.4,-0.7,-16.1)m, (0.4,-0.7,-15.1)m, (0.4,-0.7,-12)m, (0.4,-0.7,0)m, and (0.4,-0.7,+15.1m). These positions were selected to probe near the edge of the fiducial volume ($\pm$16.1m). Figure 4 shows the observed vertex distributions and Table I gives the efficiencies at 3 MeV and 4 MeV. Comparing ϵ_{fit} of just the last stage (due to the resolution of the fast fit with respect to the maximum likelihood fit) shown in the first two efficiency columns to the overall efficiency ϵ, the WIT inefficiency is mostly due to vertex resolution. Since the intelligent trigger system of Super-Kamiokande I-III are also built with tandem vertex fitters, they have comparable inefficiencies at those energies. (Of course, then the hardware trigger threshold never allowed 3 MeV events.)

VII. DAY/NIGHT ASYMMETRY

The solar neutrino oscillation parameters predict a fairly small day/night asymmetry (about 1.5%). To eventually measure such a small asymmetry requires excellent control of systematic effects and a very large data sample. The well-calibrated Super-Kamiokande detector

with its large fiducial mass of 22.5kton is at present the only detector that can probe such small asymmetries. The fit to the amplitude of the day/night variation was only performed for the Super-Kamiokande-I data (1.6% statistical uncertainty); we expect the Super-Kamiokande-II data yield a (statistical) precision of 3.4% with this method. The A_{DN} uncertainty of the Super-Kamiokande-III data should be 2.9%, so Super-Kamiokande-I/II/III combined can determine A_{DN} to $\pm 1.3\%$. The present estimate of the systematic uncertainty for Super-Kamiokande-I is 1.3%, however, it is a rather conservative estimate based on the idea of simply splitting the data into a day and a night sample. The dominant source of systematic uncertainty to day/night variation is the directional dependence of the energy scale. Multiple Coulomb scattering smears the direction of the recoil electrons by 20 to 30 degrees, so a varying energy scale can only explain slow day/night variations while at least some of the flavor conversion variation from the matter effects of the earth happens much faster. Using calibration data taken with a deuterium-tritium (DT) neutron generator (which produces ^{16}N *in situ* via a charge-exchange reaction with ^{16}O) [5] this systematic effect can be verified and understood. If this is indeed a correct description of the effect, the amplitude fit to the day/night variation would be more robust than the estimated 1.3%. So a total uncertainty of 1.4% might be reached assuming the systematic uncertainty can be reduced by 50%.

VIII. Spectral Distortion

The predicted spectral distortion in the elastic scattering rate (due to the transition of matter-driven oscillations to vacuum-driven oscillations at around 3 MeV) is on the order of 10% in the energy region 4 to 15 MeV. Assuming the observed background level in the central 13.3kton of Super-Kamiokande-III, a fiducial mass of 13.3 kton from 4 to 5.5 MeV, and a fiducial mass of 22.5kton for energies above 5.5 MeV, Super-Kamiokande can resolve this 10% effect within twelve years at three standard deviation significance. If we can further improve the water circulation pattern to suppress Radon transport to take advantage of the full fiducial mass of 22.5ktons for all energies, the same significance will be achieved in ten years. The energy-bin correlated systematic uncertainties are rather important for the spectral sensitivity: if they can be reduced by 50%, the same significance is reached within eight years (assuming full fiducial mass at all energies). This systematics is mostly limited by position dependence of the Super-Kamiokande energy scale. This energy scale is defined by injecting single, downward-going electrons into Super-Kamiokande with an electron linear accelerator [6]. The energy can be tuned between 4.5 and 16.5 Mev. In addition, the DT neutron generator data also defines the energy scale at a single energy, but uniform in direction, with higher statistics, and at more positions. Furthermore, various laser light injectors at different wavelength help with understanding the optical properties of the detector to better control energy-scale related systematic uncertainties.

IX. Conclusion

Even in the thirteenth year of measuring solar neutrinos, Super-Kamiokande still impacts solar neutrino physics. The new, threshold-less electronics and data acquisition system in conjunction with better calibration and control of systematic effects will help reveal the role of solar and terrestrial matter effects in solar neutrino oscillations.

References

[1] Q. R. Ahmad et al., **Phys. Rev. Lett.87: 071301**, (2001)
[2] J. Hosaka et al., **Phys.Rev.D73: 112001**, (2006)
[3] J. P. Cravens et al., **Phys.Rev.D78: 032002**, (2008)
[4] S. P. Mikheyev and A. Y. Smirnov, **Sov. Jour. Nucl. Phys. 42: 913** (1985); L. Wolfenstein, **Phys.Rev.D17: 2369**, (1978)
[5] E. Blaufuss et al., **Nucl.Instrum.Meth.A458: 638**, (2001)
[6] M. Nakahata et al., **Nucl.Instrum.Meth.A421: 113**, (1999)